Fe(III)-Coordination Properties of Neuromelanin Components: 5,6-Dihydroxyindole and 5,6-Dihydroxyindole-2-carboxylic Acid

Louise K. Charkoudian and Katherine J. Franz*

Department of Chemistry, Duke University, P.O. Box 90346, Durham, North Carolina 27708

Received January 4, 2006

The Fe(III)-coordination chemistry of neuromelanin building-block compounds, 5,6-dihydroxyindole (DHI), 5,6-dihydroxyindole-2-carboxylic acid (DHICA), and 5,6-dihydroxy-*N*-methyl-indole (Me-DHI), and the neurotransmitter dopamine were explored in aqueous solution by anaerobic pH-dependent spectrophotometric titrations. The Fe-(III)-binding constants and pH-dependent speciation parallel those of catechol in that mono, bis, and tris FeL_x species are present at concentrations dependent on the pH. The bis FeL_2 dihydroxyindole species are favorable for L = DHI and DHICA under neutral to mildly acidic conditions. DHI and DHICA are stronger Fe(III) chelates than catechol, dopamine, and Me-DHI at pH values from 3 to 10. Oxidation studies reveal that iron accelerates the air oxidation of DHI and DHICA.

Introduction

A striking characteristic of Parkinson's disease is the selective degeneration of dopaminergic neurons containing neuromelanin (NM), a partially defined insoluble black pigment that accumulates in the substantia nigra and locus coeruleus of healthy brains with age.[1,2] In humans, NM pigmentation increases steadily over a lifetime, appearing around age three and approaching 4 μg of NM/mg of substantia nigra tissue by age eighty.[3,4] In Parkinson's disease, however, the NM concentration diminishes below 50% of age-matched controls,[4] while concurrently, the total iron concentration within the diseased substantia nigra increases up to 35%.[5−9] Because redox-active iron can catalyze the production of damaging hydroxyl radicals through Fenton chemistry, this elevated iron load has been proposed as a contributor to neurodegeneration via iron-stimulated oxidative damage.[10−12]

The redox activity of melanins is generally thought to contribute to their free radical scavenging ability.[13,14] In addition, NM has a high capacity to sequester metal ions, particularly iron.[15−18] This property may therefore impart an additional protective role to the pigment,[19−22] since healthy

* To whom correspondence should be addressed. E-mail: katherine.franz@duke.edu.

(1) Zucca, F.; Giaveri, G.; Gallorini, M.; Albertini, A.; Toscani, M.; Pezzoli, G.; Lucius, R.; Wilms, H.; Sulzer, D.; Ito, S.; Wakamatsu, K.; Zecca, L. *Pigm. Cell Res.* **2004**, *17*, 610−616.

(2) Fedorow, H.; Tribl, F.; Halliday, G.; Gerlach, M.; Riederer, P.; Double, K. L. *Prog. Neurobiol.* **2005**, *75*, 109−124.

(3) Zecca, L.; Gallorini, M.; Schünemann, V.; Trautwein, A. X.; Gerlach, M.; Riederer, P.; Vezzoni, P.; Tampellini, D. *J. Neurochem.* **2001**, *76*, 1766−1773.

(4) Zecca, L.; Fariello, R.; Riederer, P.; Sulzer, D.; Gatti, A.; Tampellini, D. *FEBS Lett.* **2002**, *510*, 216−220.

(5) Dexter, D. T.; Wells, F. R.; Lees, A. J.; Agid, F.; Agid, Y.; Jenner, P.; Marsden, C. D. *J. Neurochem.* **1989**, *52*, 1830−1836.

(6) Graham, J. M.; Paley, M. N. J.; Grünewald, R. A.; Hoggard, N.; Griffiths, P. D. *Brain* **2000**, *123*, 2423−2431.

(7) Sofic, E.; Paulus, W.; Jellinger, K.; Riederer, P.; Youdim, M. B. H. *J. Neurochem.* **1991**, *56*, 978−982.

(8) Thong, P. S. P.; Watt, F.; Ponraj, D.; Leong, S. K.; He, Y.; Lee, T. K. Y. *Nucl. Instrum. Methods Phys. Res., Sect. B.* **1999**, *158*, 349−355.

(9) Dexter, D. T.; Carayon, A.; Javoy-Agid, F.; Agid, Y.; Wells, F. R.; Daniel, S. E.; Lees, A. J.; Jenner, P.; Marsden, C. D. *Brain* **1991**, *114*, 1953−1975.

(10) Berg, D.; Gerlach, M.; Youdim, M. B. H.; Double, K. L.; Zecca, L.; Riederer, P.; Becker, G. *J. Neurochem.* **2001**, *79*, 225−236.

(11) Zecca, L.; Stroppolo, A.; Gatti, A.; Tampellini, D.; Toscani, M.; Gallorini, M.; Giaveri, G.; Arosio, P.; Santambrogio, P.; Fariello, R. G.; Karatekin, E.; Kleinman, M. H.; Turro, N.; Hornykiewicz, O.; Zucca, F. A. *Proc. Natl. Acad. Sci., U.S.A.* **2004**, *101*, 9843−9848.

(12) Zecca, L.; Youdim, M. H.; Riederer, P.; Conner, J. R.; Crichton, R. R. *Nature Rev.* **2004**, *5*, 863−873.

(13) Ròzanowska, M.; Sarna, T.; Land, E. J.; Truscott, T. G. *Free Radical Biol. Med.* **1999**, *26*, 518−525.

(14) Samokhvalov, A.; Hong, L.; Liu, Y.; Garguilo, J.; Nemanich, R. J.; Edwards, G. S.; Simon, J. D. *Photochem. Photobiol.* **2005**, *81*, 145−148.

(15) Liu, Y.; Hong, L.; Kempf, V. R.; Wakamatsu, K.; Ito, S.; Simon, J. D. *Pigm. Cell Res.* **2004**, *17*, 262−269.

(16) Zecca, L.; Pietra, R.; Goj, C.; Mecacci, C.; Radice, D.; Sabbioni, E. *J. Neurochem.* **1994**, *62*, 1097−1101.

(17) Zecca, L.; Tampellini, D.; Gatti, A.; Crippa, R.; Eisner, M.; Sulzer, D.; Ito, S.; Fariello, R.; Gallorini, M. *J. Neural Transm.* **2002**, *109*, 663−672.

(18) Zecca, L.; Zucca, F. A.; Toscani, M.; Adorni, F.; Giaveri, G.; Rizzio, E.; Gallorini, M. *J. Radioanal. Nucl. Chem.* **2005**, *263*, 733−737.

(19) Faucheux, B. A.; Martin, M. E.; Beaumont, C.; Hauw, J. J.; Agid, Y.; Hirsch, E. C. *J. Neurochem.* **2003**, *86*, 1142−1148.

(20) Faucheux, B. A.; Martin, M. E.; Beaumont, C.; Hunot, S.; Hauw, J. J.; Agid, Y.; Hirsch, E. C. *J. Neurochem.* **2002**, *83*, 320−330.

NM is estimated to be only 50% saturated with iron and therefore maintains a potentially important chelating capacity to protect neurons against iron-promoted oxidative stress.[1,23−25] The combination of decreased NM and increased iron in Parkinson's disease implies that the protective, high-affinity iron-binding sites within NM become saturated, leaving any residual iron as "free" or bound in low-affinity sites that may retain the ability to promote Fenton chemistry and oxidative stress.[11,26] The characterization of iron complexes that represent both high-affinity and low-affinity sites of NM and the understanding of their oxidation reactivity are therefore important goals for understanding the role of iron in neurodegeneration.

Although the connectivity and three-dimensional structure of NM is unknown, there is strong evidence from chemical degradation studies that it is a polymer composed of 5,6-dihydroxyindole (DHI), 5,6-dihydroxyindole-2-carboxylic acid (DHICA), and benzothiazine units, together with lipid and protein components.[24,27,28] NM appears chemically similar to eumelanin and pheomelanin found in hair and skin, although the structural characterization of these pigments is likewise limited.[29] The chemical structures of the molecular precursors to these pigments are shown in Figure 1. The tyrosinase-dependent biosynthesis of the brown/black eumelanin pigment diverges in the presence of excess cysteine to produce cysteinyldopa and the benzothiazine intermediates of the reddish pheomelanin pigments. Although NM biosynthesis may also be enzyme driven, tyrosinase has not been detected in the substantia nigra,[2] which furthermore remains normally pigmented in albinos who lack tyrosinase.[1] Alternative enzymes have been sought but not confirmed, and a recent in vitro study suggests that NM is produced nonenzymatically via iron-mediated oxidation and polymerization of L-dopa.[30]

Potential metal-binding sites within the NM polymer include catechol, carboxylic acid, and benzothiazine functionalities, although the catechol sites have received the most attention. The semiquinone, quinone, and the quinone-imine forms of the dihydroxyindoles can also bind metal ions.[31] X-ray absorption[32] and infrared spectroscopies[33] confirm that the iron in NM is coordinated by the dihydroxy catechol
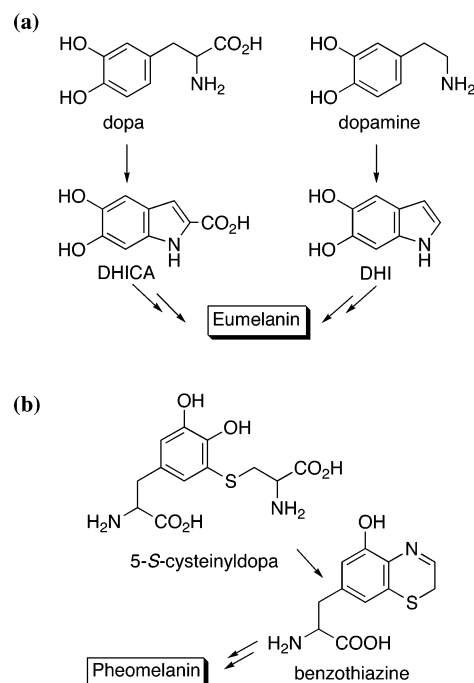

Figure 1. Black eumelanin pigments are composed of polymers of DHI and DHICA (a), whereas red pheomelanin pigments contain polymers of benzothiazine-type units (b). Neuromelanin appears to be a mixed melanin containing features of both eumelanin and pheomelanin.

groups of DHI and DHICA. Both Mössbauer[34,35] and EPR[36] studies identify Fe(III)-oxo/hydroxy clusters, which suggest that NM may provide a template for iron mineralization similar to that found in the iron storage protein ferritin. Although other studies dispute this model,[32] such clusters may represent the high-affinity sites that stabilize Fe(III), whereas low-affinity sites could be envisioned as discrete catechol-containing units on the periphery of the granule. Simple model complexes of the precursor components DHI and DHICA may reasonably model these outer sites.

Further structural information and iron-binding properties of NM (and other melanins in general) have not been fully resolved in part because of its insolubility, complications associated with its extraction and purification, and the lack of model complexes that would help decipher its structure and properties. Synthetic NM analogues produced via air or tyrosinase-catalyzed oxidation of dopamine and cysteine[21,32] lack structural identification and are easily differentiated from native samples.[34,32,37] Despite these obstacles, it remains of great interest to understand iron−NM interactions because of the possible role of iron in NM biosynthesis, as well as the role of NM in iron homeostasis and oxidative stress within the substantia nigra.

(21) Zaréba, M.; Bober, A.; Korytowski, W.; Zecca, L.; Sarna, T. *Biochim. Biophys. Acta* **1995**, *1271*, 343−348.

(22) Zecca, L.; Zucca, F. A.; Wilms, H.; Sulzer, D. *Trends Neurosci.* **2003**, *26*, 578−580.

(23) Shima, T.; Sarna, T.; Swartz, H. M.; Stroppolo, A.; Gerbasi, R.; Zecca, L. *Free Radical Biol. Med.* **1997**, *23*, 110−119.

(24) Zecca, L.; Tampellini, D.; Gerlach, M.; Riederer, P.; Fariello, R.; Sultzer, D. *J. Clin. Pathol.: Mol. Pathol.* **2001**, *54*, 414−418.

(25) Linert, W.; Herlinger, E.; Jameson, R. F.; Kienzl, E.; Jellinger, K.; Youdim, M. B. H. *Biochim. Biophys. Acta* **1996**, *1316*, 160−168.

(26) Double, K. L.; Ben-Shachar, D.; Youdim, M. B. H.; Zecca, L.; Riederer, P.; Gerlach, M. *Neurotoxicol. Teratol.* **2002**, *24*, 621−628.

(27) Odh, G.; Carstam, R.; Paulson, J.; Wittbjer, A.; Rosengren, E.; Rorsman, H. *J. Neurochem.* **1994**, *62*, 2030−2036.

(28) Double, K. L.; Zecca, L.; Costi, P.; Mauer, M.; Griesinger, C.; Ito, S.; Ben-Shachar, D.; Bringmann, G.; Fariello, R. G.; Riederer, P.; Gerlach, M. *J. Neurochem.* **2000**, *75*, 2583−2589.

(29) Ito, S. *Pigm. Cell Res.* **2003**, *16*, 230−236.

(30) Sulzer, D.; Bogulavsky, J.; Larsen, K. E.; Behr, G.; Karatekin, E.; Kleinman, M. H.; Turro, N.; Krantz, D.; Edwards, R. H.; Greene, L. A.; Zecca, L. *Proc. Natl. Acad. Sci. U.S.A.* **2000**, *97*, 11869−11874.

(31) Szpoganicz, B.; Gidanian, S.; Kong, P.; Farmer, P. *J. Inorg. Biochem.* **2002**, *89*, 45−53.

(32) Kropf, A. J.; Bunker, B. A.; Eisner, M.; Moss, S. C.; Zecca, L.; Stroppolo, A.; Crippa, P. R. *Biophys. J.* **1998**, *75*, 3135−3142.

(33) Bridelli, M. G.; Tampellini, D.; Zecca, L. *FEBS Lett.* **1999**, *457*, 18−22.

(34) Gerlach, M.; Trautwein, A. X.; Zecca, L.; Youdim, M. B. H.; Riederer, P. *J. Neurochem.* **1995**, *65*, 923−926.

(35) Galazka-Friedman, J.; Bauminger, E. R.; Koziorowski, D.; Friedman, A. *Biochim. Biophys. Acta* **2004**, *1688*, 130−136.

(36) Aime, S.; Bergamasco, B.; Biglino, D.; Digilio, G.; Fasano, M.; Giamello, E.; Lopiano, L. *Biochim. Biophys. Acta* **1997**, *1361*, 49−58.

(37) Bolzoni, F.; Giraudo, S.; Lopiano, L.; Bergamasco, B.; Fasano, M.; Crippa, P. R. *Biochim. Biophys. Acta* **2002**, *1586*, 210−218.

The current study characterizes and compares the iron-binding properties of the NM precursor, dopamine, and the principal building blocks of the NM pigment, DHI and DHICA. The *N*-methylated derivative Me-DHI is also included.

Experimental Section

Materials and Instrumentation. Chemicals were obtained from Fisher Scientific and used without further purification unless otherwise noted. All solvents were reagent grade and all aqueous solutions were prepared from Nanopure-quality water. UV−vis spectra were recorded on a Photonics Model 420 Fiber Optic CCD Array UV−vis spectrophotometer. ^{1}H and ^{13}C NMR spectra were recorded on a Varian Inova 400 spectrometer. Electrospray ionization mass spectrometry (ESI-MS) was performed on an Agilent 1100 Series LC/MSD trap spectrometer with a Daly conversion dynode detector. Samples were infused via a Harvard Apparatus syringe pump at 33 μL/min. Ionization was achieved in the positive- or negative-ion mode by application of +5 or −5 kV at the entrance to the capillary; the pressure of the nebulizer gas was 20 psi. The drying gas was heated to 325 °C at a flow of 7 L/min. Full-scan mass spectra were recorded in the mass/charge (*m/z*) range of 50−2000. Elemental analysis was performed by Desert Analytics, Tucson, AZ.

Fe(III) perchlorate solutions (0.1 M) were prepared from recrystallized Fe(III) perchlorate and standardized spectrophotometrically in strong acid.[38] NaOH, HClO$_4$, and NaClO$_4$ solutions (0.5 M, 0.01 M, 0.1 M, respectively) were prepared with boiled deionized water and were degassed upon cooling to remove carbonate. NaOH solutions were standardized by titration with both 0.2 M HCl and potassium hydrogen phthalate to a phenolphthalein end point and were stored under N$_2$; HClO$_4$ stock solutions were prepared from concentrated perchloric acid and were standardized by titration with standard NaOH to a phenolphthalein end point. All solutions were degassed with N$_2$ or Ar for 45 min prior to each experimental run.

Potentiometric and Spectrophotometric Titrations. All titrations were carried out at 22 °C with stirring, and all titration solutions had an initial volume of 25.0 mL. A Schott Titronic 110 *plus* autotitrator kept under constant Ar sparge was used to deliver 10 to 500 μL of acid or base through a gastight titrator tip. The titration vessel consisted of a foil-covered 50 mL 4-neck round-bottom flask equipped with a pH probe (Orion combination pH electrode model 8103BN filled with 3 M NaCl), a UV−vis probe (Photonics dual source dip probe), a titrator buret tip, a gas inlet, and a bubbler outlet. A positive flow of Ar preserved the inert atmosphere necessary for these titrations. The glass-bulb probe was calibrated by the standard method for pH values of 3−11 and by the junction-potential method for pH values below 3, according to the instructions provided in the Hyperquad software package.[39] The concentration of NaClO$_4$ supporting electrolyte was 0.1 M for all titrations. Measurements were recorded for each data point with the stir bar off and only after the pH equilibrated to a constant value for several minutes. All pK_a and β values were the average of three or more titrations and were calculated using Hyperquad software.[39,40] Further details of the data-fitting procedures are included in Supporting Information.

Synthesis. 5,6-Dihydroxyindole (DHI). DHI was prepared under strict inert conditions by a procedure similar to that described by Wakamatsu and Ito.[41] A solution of K$_3$[Fe(CN)$_6$] (6.6 g, 20 mmol) and NaHCO$_3$ (2.5 g, 30 mmol) in H$_2$O (60 mL) was added over the course of 5 min to a stirred solution of DL-dopa (0.99 g, 5 mmol) in 500 mL H$_2$O. The wine-red solution was kept at room temperature for 3 h and was then extracted with ethyl acetate (250 mL × 3). The combined ethyl acetate extracts were washed with a saturated NaCl solution containing 3.0 g of Na$_2$S$_2$O$_5$ (100 mL × 3) and were dried over Na$_2$SO$_4$. Evaporation gave a pale brown solid, which was recrystallized from benzene−hexane to give 287 mg (39% yield) of DHI as pale yellow crystals. ^{1}H NMR (CD$_3$-OCD$_3$): δ 6.216 (1H, t), 6.78 (1H, s), 6.918 (1H, s), 7.05 (1H, m,), 7.36 (1H, m). Anal. Calcd for C$_8$H$_7$NO$_2$: C, 64.42; H, 4.73; N: 9.39. Found: C, 64.64; H, 4.57; N, 9.25.

5,6-Dihydroxyindole-2-carboxylic acid (DHICA). DHICA was prepared under strict inert conditions by a procedure similar to that described by Wakamatsu and Ito.[41] A solution of K$_3$[Fe(CN)$_6$] (6.6 g, 20 mmol) and NaHCO$_3$ (2.5 g, 30 mmol) in H$_2$O (60 mL) was added over the course of 5 min to a stirred solution of DL-dopa (0.99 g, 5 mmol) in 500 mL H$_2$O. NaOH (1 M, 70 mL) was added to the wine-red solution. After it was stirred for 15 min, the reaction mixture was quenched with HCl (6 M HCl) and extracted with ethyl acetate (3 × 250 mL). The combined ethyl acetate extracts were washed with a saturated NaCl solution (100 mL) containing 0.19 g (1 mmol) of Na$_2$S$_2$O$_5$ and a saturated NaCl solution (100 mL × 2) and then dried over Na$_2$SO$_4$. Evaporation gave a brown oil, which was dissolved in acetone (25 mL). The addition of hexanes (100 mL) gave a brown oil, which was discarded. Further addition of hexanes (150 mL) yielded 410 mg (42%) of DHICA as a white powder. Anal. Calcd for C$_9$H$_7$NO$_4$: C, 55.96; H, 3.70; N: 7.05. Found: C, 55.62; H, 3.86; N: 6.83. ^{1}H NMR (CD$_3$-OCD$_3$): δ 6.96 (t, 2H, *J* = 1), 7.03 (s, 1H), 10.35 (s, 1H).

5,6-Dihydroxy-*N*-methyl-indole (Me-DHI). Me-DHI was prepared under strict inert conditions by a procedure similar to that described by Corradoini and Prota.[42] A solution of K$_3$[Fe(CN)$_6$] (13 g, 39.5 mmol) and NaHCO$_3$ (4.2 g, 9.5 mmol) in 50 mL H$_2$O was added to a solution of epinephrine (1.3 g, 7.5 mmol) and tartaric acid (2.24 g, 14.9 mmol) in 25 mL H$_2$O under vigorous stirring. After the reaction mixture was stirred for 5 min, 150 mL of peroxide-free ethyl ether was added to it. Scoops of ascorbic acid were added until the red color dissipated. The aqueous layer was extracted with diethyl ether (3 × 100 mL). The organic layers were washed with brine (1 × 100 mL) and dried over sodium sulfate. Evaporation of the solvent under N$_2$ afforded a yellow solid, which was recrystallized from ether−benzene to give pale yellow needles (650 mg) in a 55% yield. ^{1}H NMR (CDCl$_3$): δ 3.67 (3H, s), 4.82 (1H, s), 5.31 (1H, s), 6.28 (1H, d, *J* = 2.90), 6.82 (1H, s), 6.88 (1H, d, *J* = 3.08), 7.04 (1H, s). Anal. Calcd for C$_9$H$_9$NO$_2$: C, 66.01; H, 5.55; N: 8.64. Found: C, 66.33; H, 5.71; N: 8.36.

Results

Ligand pK_a Determination. The acid association constants K_{an}^H (*n* = 1, 2, 3) of the ligands investigated in this study are defined by eqs 1 and 2. Their values, which were determined from a combination of potentiometric and spectrophotometric titrations, are listed in Table 1 as pK_{an} (−log K_{an}^H). All the ligands contain a dihydroxybenzene core of

(38) Bastian, R.; Weberling, R.; Palilla, F. *Anal. Chem.* **1956**, *28*, 459−462.

(39) Gans, P.; Sabatini, A.; Vacca, A. *Hyperquad2000*; Protonic Software: Leeds, U.K., 2000.

(40) Gans, P.; Sabatini, A.; Vacca, A. *Talanta* **1996**, *43*, 1739−1753.

(41) Wakamatsu, K.; Ito, S. *Anal. Biochem.* **1988**, *170*, 335−340.

(42) Corradoini, M. G.; Napolitano, A.; Prota, G. *Tetrahedron* **1986**, *42*, 2083−2088.

Table 1. Ligand Protonation Constants and Fe(III) Stability Constants

	ligand				
	Catechol	Dopamine	DHI	Me-DHI	DHICA
$pK_{a1}{}^a$	9.24(6)	9.59(4)	9.54(2)	9.65(5)	9.76(4)
$pK_{a2}{}^b$	13.0(1)	13.11(9)	13.09(4)	13.14(3)	13.2(1)
$pK_{aR}{}^a$					4.25(6)
$pK_{aN}{}^b$		10.14(5)			
$\log \beta_{110}{}^c$	20.05(4)	21.63(1)	21.9 (1)	21.57(6)	21.8(1)
$\log \beta_{120}{}^c$	34.71(3)	35.02(6)	38.89(9)	37.28(8)	39.75(4)
$\log \beta_{130}{}^c$	43.75(5)	45.8(1)	49.19(9)	45.4 (5)	50.33(6)
pFe^d	14.4	14.1	17.6	15.7	17.8

^{a} Determined by anaerobic potentiometric titration: $C_L = 1.00$ mM, $\mu = 0.1$ M NaClO$_4$, 22 °C, pH range = 1.0−10.5. ^{b} Determined by anaerobic spectrophotometric titrations: $C_L = 1.00$ mM, $\mu = 0.1$ M NaClO$_4$, 22 °C, pH range 7.0−14 with upper pH limit estimated by total moles base added during spectrophotometric titration. ^{c} Determined from a combination of potentiometric and spectrophotometric titrations: $C_L = 0.48$ mM, $C_{Fe} = 0.13$ mM, pH = 3.0−10.0, 22 °C, $\mu = 0.1$ M NaClO$_4$. ^{d} Calculated for $[Fe(III)]_{tot} = 10^{-6}$ M, $[L]_{tot} = 10^{-5}$ M, and pH = 7.4.

catechol, while dopamine and DHICA both have an additional ionizable proton on their amine and carboxylic acid groups, respectively. The pK_a values of the indole amines on DHI and DHICA are estimated to be beyond the 3−10 pH range of our experiments; therefore, DHI and Me-DHI were both treated as diprotic acids ($n = 2$), while DHICA and dopamine were treated as triprotic acids ($n = 3$) for data analysis. Figure 2a displays the pH titration curves of dopamine, Me-DHI, DHI, and DHICA as a function of the molar ratio, a, of added base per ligand; catechol was also investigated for comparison but is not included in the figure. Deprotonation of the carboxylic acid on DHICA gives rise to the buffer region at low pH in Figure 2a, shifting its inflection point to a higher a value than the other ligands. These potentiometric titrations were used to obtain the first pK_a values, whereas spectrophotometric data were required to accurately determine the higher pK_a values. Our results for catechol[43,44] and dopamine[45,46] agree with previously published reports. As expected, the ligand pK_a values of the NM precursors are similar to those of catechol.

$$H_{n-1}L + H^+ \rightleftharpoons H_nL \qquad (1)$$

$$K_{an}^H = \frac{[H_nL]}{[H_{n-1}L][H^+]} \qquad (2)$$

Fe(III) Complex Formation. Figure 2b displays the anaerobic potentiometric titration curves of dopamine, DHI, DHICA, and Me-DHI carried out in the presence of Fe(III) at a ligand/metal ratio in excess of 3:1. The m value is the ratio of moles base added per mole of iron. The titrations are reversible when carried out in either direction, going from high to low or from low to high pH, verifying that the Fe(III)−ligand complexes are in equilibrium. A small amount of purple precipitate that forms when the titrations start at
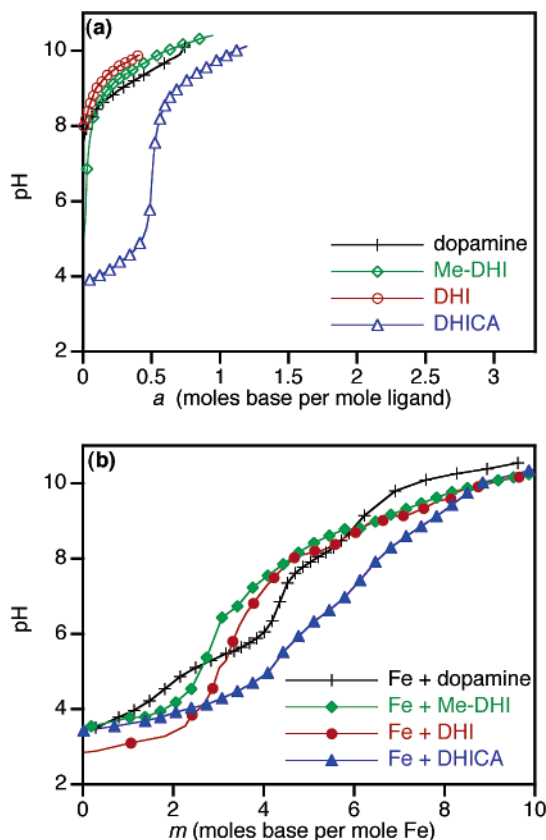
(43) Avdeef, A.; Sofen, S. R.; Bregante, T. L.; Raymond, K. N. *J. Am. Chem. Soc.* **1978**, *100*, 5362−5370.
(44) Howlin, B.; Mohd-Nor, A. R.; Silver, J. *Inorg. Chim. Acta* **1984**, *91*, 153−160.
(45) Gerard, C.; Chehhal, H.; Hugel, R. P. *Polyhedron* **1994**, *13*, 591−597.
(46) Kiss, T.; Gergely, A. *Inorg. Chim. Acta* **1979**, *36*, 31−36.

Figure 2. (a) Potentiometric titration curves of dopamine, Me-DHI, DHI, and DHICA vs a, where $a = (C_B − C_A)/C_L$: C_B represents the moles of base added during the titration, C_A respresents the moles of acid added initially, and $C_L = 1.0$ mM. (b) Potentiometric titration curves of ligands and Fe(III) vs m, where $m = (C_B − C_A)/C_{Fe}$: $C_{Fe} = 0.13$ mM and $C_L = 0.48$ mM. T = 22 °C, $\mu = 0.1$ M NaClO$_4$. For comparison between plots a and b, $m = 3a$.

low pH redissolves as the titration progresses to basic pH. This purple precipitate is a neutral or insoluble iron species that has been observed in other Fe(III) catechol-type systems,[47] and it can be avoided altogether by titrating the solution from high to low pH.

The Fe(III)−dopamine titration is included in Figure 2b as a reference to which the dihydroxyindole ligands can be compared. In agreement with previous studies, its curve shows three distinct steps that each correspond to the release of two protons upon Fe(III) binding.[45,48] For triprotic dopamine (H_3L^+), these three steps point to formation of the mono species $Fe(HL)^{2+}$ at pH values below 5.7, the bis species $Fe(HL)_2^+$ at pH values between 5.7 and 7.2, and the tris species $Fe(HL)_3$ above pH 7.3, with further deprotonation of $Fe(HL)_3$ occurring above pH 10.[45] In contrast, the potentiometric curves of the dihydroxyindole ligands Me-DHI, DHI, and DHICA in the presence of Fe(III) exhibit a rather smooth and steady increase in pH over the course of the titration. Diprotic DHI and Me-DHI (H_2L) both show a buffer region below $m = 2$ that indicates formation of mono $Fe(L)^+$ species, followed by a steady increase in pH from m

(47) Dhungana, S.; Heggemann, S.; Heinisch, L.; Möllmann, U.; Boukhalfa, H.; Crumbliss, A. L. *Inorg. Chem.* **2001**, *40*, 7079−7086.
(48) Crisponi, G.; Lai, A.; Monduzzi, M.; Saba, G. *Inorg. Chim. Acta* **1983**, *80*, 85−88.
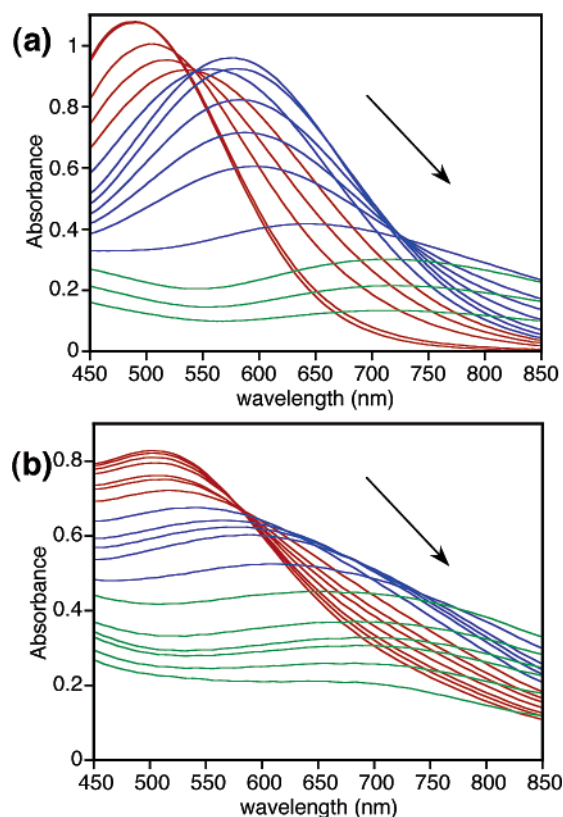
Figure 3. pH-dependent anaerobic spectrophotometric titrations of (a) Fe-(III) + dopamine and (b) Fe(III) + DHI. Conditions: $C_L = 0.48$ mM, $C_{Fe(III)} = 0.13$ mM, 22 °C, and $\mu = 0.1$ M NaClO$_4$. Arrows represent decreasing pH from 10.00 to 3.00.

Table 2. Wavelength and Extinction Coefficients for Mono, Bis, and Tris Fe(III)L$_x$ Species Extracted from the Anaerobic pH-dependent Spectrophotometric Titrations[a]

	FeL		FeL$_2$		FeL$_3$	
ligand	λ_{max} $(\epsilon)^b$	pH	λ_{max}, $(\epsilon)^b$	pH	λ_{max}, $(\epsilon)^b$	pH
catechol	723 (4626)	3–4.8	574 (8308)	4.8–7.8	474 (9692)	>7.8
dopamine	736 (2777)	3–5.7	581 (7177)	5.7–7.2	493 (9154)	>7.3
DHI	654 (4155)	3–3.9	588 (5368)	3.4–7.4	513 (6338)	>7.4
Me-DHI	614 (5308)	3–4.6	550 (7485)	4.6–8.6	499 (9731)	>8.6
DHICA	637 (2958)	3–3.8	587 (7670)	3.8–7.4	516 (10865)	>7.4

[a] The pH range indicates the calculated pH values in which that species predominates. Conditions: $C_L = 0.48$ mM, $C_{Fe(III)} = 0.13$ mM, pH = 3.0–10.0, 22 °C, $\mu = 0.1$ M NaClO$_4$. [b] λ_{max} in nm and ϵ in M^{-1} cm^{-1}.

= 2 to 6 without noticeable buffer regions for the formation of the bis and tris Fe(L)$_2^-$ and Fe(L$_3$)$^{3-}$ complexes. DHICA (H$_3$L) in the presence of Fe(III) behaves similarly to DHI and Me-DHI with a steady increase in pH through the formation of the tris Fe(L)$_3^{6-}$ complex, but the curve shifts to a higher *m* value to account for the deprotonation of the carboxylic acid.

Intense ligand-to-metal charge transfer (LMCT) bands of the iron complexes allow the proton-dependent equilibria to be monitored spectrophotometrically. Figure 3 displays the changes in the visible spectra of dopamine and DHI with Fe(III) at a ligand/metal ratio of 3.7:1 as the pH is steadily adjusting from 10 to 3. The spectral profiles of DHICA and Me-DHI with Fe(III) are similar to the DHI example in Figure 3 and are included in the Supporting Information.

All of the ligands examined display at least three spectrophotometrically distinguishable species that can be assigned by comparison to the well-defined Fe(III)−catechol system.[44,43,49−52] For the sake of generality, we will use the FeL$_x$ notation without parentheses to ignore the charge state of the complexes, which varies across our series of ligands. In all cases, a red complex corresponding to tris FeL$_3$ forms under alkaline conditions. Upon addition of acid, a blue species indicative of bis FeL$_2$ predominates, which converts under more acidic conditions to a green complex that is assigned as mono FeL. The titrations are completely reversible upon the addition of base, verifying that pH-dependent equilibria exist among the FeL$_x$ complexes. The major difference in the iron-binding spectral profiles between the

dihydroxyindole ligands and dopamine is the relatively subtle profile of the blue bis species for the dihydroxyindoles, as can be seen by comparing the spectra in Figure 3. This pattern mirrors the results from the potentiometric data, where distinct steps in the potentiometric curves are observed only for the Fe−dopamine case.

The Fe−DHICA system exhibits a fourth spectrophotometrically distinguishable species between pH 2.3 and 3.6 that is not seen with the other ligands. A purple color with $\lambda_{max} = 516$ nm appears when titrating from low pH to high pH but is not seen when the pH is adjusted from high to low. The species remains in solution and is distinct from the dark, insoluble purple precipitate that is observed in all cases and discussed above. We speculate that this species corresponds to binding of the carboxylic acid functionality of DHICA to Fe(III).

To observe the equilibrium between [Fe(OH$_2$)$_6$]$^{3+}$ and mono FeL, a second set of titrations was carried out from pH 2.5 to 1.0 for each ligand. Under such acidic conditions, protons released upon metal chelation contribute insignificantly to the pH measurement, therefore these titrations were monitored solely by spectrophotometric readings (not shown), which were fit in Hyperquad to a model containing [Fe(OH$_2$)$_6$]$^{3+}$, FeL, and FeHL species. As the pH is lowered, the intensity of the LMCT band at $\lambda_{max} \approx 700$ nm for the mono FeL species decreases. This behavior is consistent with protonation of FeL to FeHL and dissociation of the ligand from the metal. The low pH also favors an internal electron transfer to give Fe(II) and semiquinone.[43,53−55]

The specific speciation and the LMCT band wavelengths with their corresponding extinction coefficients for each FeL$_x$ spectral profile are compiled in Table 2. Further characterization of the FeL$_x$ speciation was obtained by analyzing the solutions of the Me-DHI system at specific pH values by electrospray ionization mass spectrometry (ESI-MS) under

(49) Sever, M. J.; Wilker, J. J. *J. Chem. Soc., Dalton Trans.* **2004**, 1061−1072.
(50) Karpishin, T. B.; Gebhard, M. S.; Solomon, E. I.; Raymond, K. N. *J. Am. Chem. Soc.* **1991**, *113*, 2977−2984.
(51) Nardillo, A. M. *J. Inorg. Nucl. Chem.* **1981**, *43*, 620−624.
(52) Mentasti, E.; Pelizzetti, E. *J. Chem. Soc., Dalton Trans.* **1973**, 2605−2608.
(53) Hynes, M. J.; O'Coinceanainn, M. *J. Inorg. Biochem.* **2004**, *98*, 1457−1464.
(54) El-Ayaan, U.; Herlinger, E.; Jameson, R. F.; Linert, W. *J. Chem. Soc., Dalton Trans.* **1997**, 2813−2818.
(55) Linert, W.; Jameson, R. F.; Herlinger, E. *Inorg. Chim. Acta* **1991**, *187*, 239−247.

inert conditions. The most prominent signal observed in the negative mode for the blue species at pH 7.5 occurs at $m/z = 377.9$, which is consistent with $[Fe(Me-DHI)_2]^{-1}$ with a molecular formula of $FeC_{18}H_{14}N_2O_4$ with a calculated mass of 378.19. This species can pick up two protons to give a calculated mass of 380.19 for $FeC_{18}H_{16}N_2O_4$, which appears as a prominent signal at $m/z = 381.1$ in the positive-mode spectrum. Analysis of the red solution at pH 10.5 by positive-mode ESI-MS revealed prominent signals at $m/z = 587.0$, 609.1, and 631.1, which are consistent with the $z = 1$ charge state of various H^+ and Na^+ adducts of $[Fe(Me-DHI)_3]^{3-}$ calculated as 587.3, 608.3, and 630.4 for $Na_2FeC_{27}H_{23}N_3O_6$, $Na_3FeC_{27}H_{22}N_3O_6$, and $Na_4FeC_{27}H_{21}N_3O_6$, respectively. In the case of DHICA, bis and tris FeL_x species were also detected by ESI-MS, but the observed masses indicated a mixture of DHICA and DHI units, suggesting decarboxylation of DHICA. We do not know at this point if the decarboxylation occurs in solution or is solely a result of the ESI-MS experiment.

The stepwise equilibria for the FeL_x complexes are represented in a general form by eq 3, where $x = 1, 2, 3$. The overall stability constants β_{110}, β_{120}, and β_{130}, defined by eq 4, were calculated from a combined analysis of the potentiometric and spectrophotometric data using Hyperquad software; the average values and their standard deviations from at least three trials are listed in Table 1. Since the model NM ligands are weak acids, protons compete with iron binding, depending on the ligand's pK_a and the pH of the solution. The β stability constants are therefore not necessarily the best measure for comparing relative binding strengths under a specific set of conditions, so Table 1 also compiles pFe values, where pFe is defined as the negative log of the free or unchelated Fe(III) in solution at pH 7.4 with a total ligand concentration of 10 μM and total Fe concentration of 1 μM.[56,57] A high pFe value indicates a stable Fe(III) chelate complex,[56] and because it does not depend on the metal–ligand stoichiometry the way β and K values do, the pFe value can be used to compare directly the binding strengths of ligands of varying denticity.

$$Fe + xL^{2-} \rightleftharpoons FeL_x \qquad (3)$$
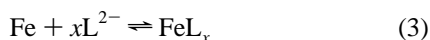
$$\beta_{1x0} = \frac{[FeL_x]}{[Fe][L^{2-}]^x} \qquad (4)$$

When the pH-dependent spectrophotometric titrations were repeated in the presence of Fe(II) rather than Fe(III), no LMCT bands were observed between pH 3 and 10. The Fe(II)–dihydroxyindole solutions react upon exposure to air to form corresponding Fe(III)–dihydroxyindole complexes that undergo subsequent oxidative polymerization to yield a brown/black precipitate.

To examine the oxidation process in more detail, solutions of DHI and DHICA at pHs 3, 7, and 9 in the absence and
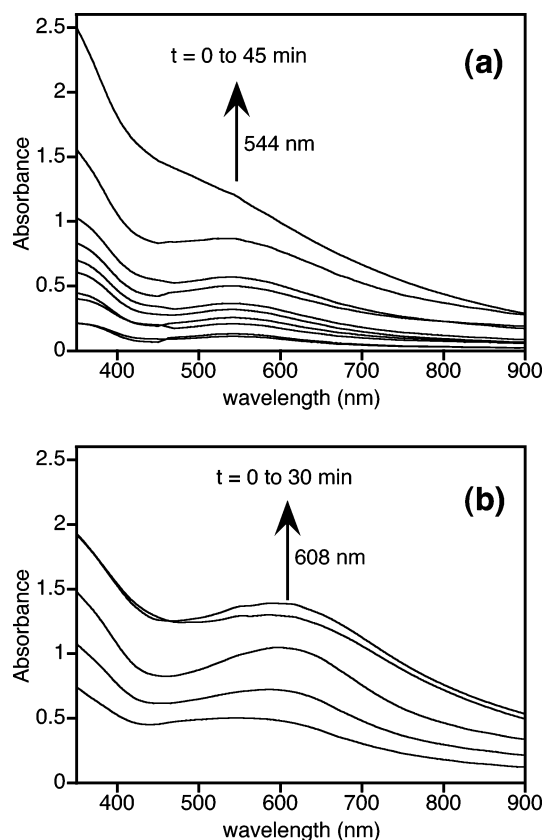

Figure 4. (a) Air oxidation of 0.48 mM DHI at pH 9 monitored for 45 minutes. (b) Air oxidation of 0.48 mM DHI and 0.13 mM Fe(III) at pH 9 monitored for 30 minutes.

presence of Fe(III) were exposed to air and monitored spectrophotometrically over time. DHI was susceptible to air oxidation at all pH values, turning a characteristic blue color with a band centered at $\lambda_{max} = 544$ nm that increases and broadens while a black precipitate forms. The spectra taken over 45 min for the oxidation of DHI at pH 9 are shown in Figure 4a. The blue chromophore is indicative of melanochrome, an intermediate observed during the enzymatic oxidation of dopa to melanin.[58] Oxidation studies of DHI by others have revealed the primary component of melanochrome to be the 2,2′-biindolyl dimer of DHI.[58] For comparison, Figure 4b shows the air oxidation of DHI in the presence of Fe(III) at a ligand/metal ratio of just over 3 and a pH of 9 to ensure formation of the tris complex, $Fe(DHI)_3^{3-}$. As with the free DHI, the spectra appear to increase and broaden along the way to formation of a black precipitate. However, in the presence of Fe(III) a distinct new band at 608 nm appears within the first minute of the reaction. This band is clearly shifted from the LMCT of $Fe(DHI)_3^{3-}$ that is centered at 505 nm and the melanochrome peak centered at 544 nm. It may be from an Fe(III) complex of melanochrome or other polymerized intermediate, but more experiments are required to confirm this assignment.

Solutions of DHICA in the absence of Fe(III) are noticeably less reactive in air than DHI, showing no spectral changes over the course of 3 h at pH 3. At neutral and basic

(56) Raymond, K. N.; Müller, G.; Matzanke, B. F., Complexation of Iron by Siderophores. In *Topics in Current Chemistry*; Boschke, F. L., Ed.; Springer-Verlag: Berlin, 1984; Vol. 123, pp 49−102.

(57) Winkelmann, G. *CRC Handbook of Microbial Iron Chelates*; CRC Press: Boston, 1991; pp 178−179.

(58) Prota, G. *Melanins and Melanogenesis*; Academic Press: San Diego, CA, 1992.

pH, melanin formation appears within about 1 h of air exposure, as revealed by a general darkening of the solution and the appearance of a black precipitate. In the presence of Fe(III), however, DHICA rapidly oxidizes at pH 3, 7, and 9 as seen by an immediate darkening of the solutions upon air exposure, followed by the formation of a black precipitate over the course of 45 min.

Discussion

Although different toxic or genetic mechanisms can initiate neuronal damage in the substantia nigra with the onset of Parkinson's disease, numerous studies link the decrease in NM and the increase in iron with a resulting increase in iron-promoted oxidative stress and neuronal death.[1,3,12] The lack of structural identification of NM inspired the current study in which we investigated the coordination chemistry between Fe(III) and various NM precursor molecules.

The electron-rich indole rings increase the basicity of the dihydroxyindole NM model ligands compared to catechol, as shown by the higher-than-9.2 pK_{a1} values of 9.54, 9.65, and 9.76 for DHI, Me-DHI, and DHICA, respectively (Table 1). The first catecholic pK_{a1} of DHICA is higher because of a negative charge on the deprotonated carboxylic acid. The second catecholic pK_{a2} for all ligands studied is around 13. Similar to the catechol system,[43,44] DHI, DHICA, Me-DHI, and dopamine form mono, bis, and tris FeL_x species with pH-dependent speciation. The binding strengths of the model NM ligands are comparable to or greater than other catechol-containing ligands and are capable of binding free Fe(III) to form stable Fe(III)−dihydroxyindole complexes. The carboxylic acid group of DHICA is able to bind weakly to Fe(III) under acidic conditions, but this complex is not in equilibrium with the Fe(III)−catecholate species. This conclusion supports previous studies on the metal-binding capacity of the eumelanin standard, squid-ink *Sepia* melanin, in which Mg(II) and Ca(II) occupy carboxylic acid binding sites, whereas Fe(III) prefers the catecholate binding sites.[15]

In skin and hair cells, melanin formation occurs within specialized acidic organelles in melanosomes that have a pH of ∼5.[58] Although the pH of the NM granules is undetermined, it is possible that they too have an acidic environment. Therefore, in addition to the standard pFe value at pH 7.4, we are also interested in judging the relative binding strengths of the NM precursors across the pH range of 3−10 examined in this study. As shown by the plot of pFe versus pH in Figure 5, DHI and DHICA are the most effective Fe(III) chelators among this group over the entire pH range. Catechol and dopamine chelate less Fe(III) than any of the dihydroxyindoles, and Me-DHI is less efficient than DHI and DHICA. At pH 5, pFe values are lower than at pH 7.4 for catechol, dopamine, DHI, DHICA, and Me-DHI with values of 9.86, 9.83, 10.42, 10.25, and 10.07, respectively. Interestingly, at neutral pH, DHICA is a more efficient Fe-(III) chelator than DHI, but at acidic pH values below 5.5, DHI is slightly stronger than DHICA. DHI and DHICA are more efficient Fe(III) chelators than their dopamine precursor over all pH values studied, indicating that oxidized metabolites of dopamine bind Fe(III) tighter than the neurotrans-
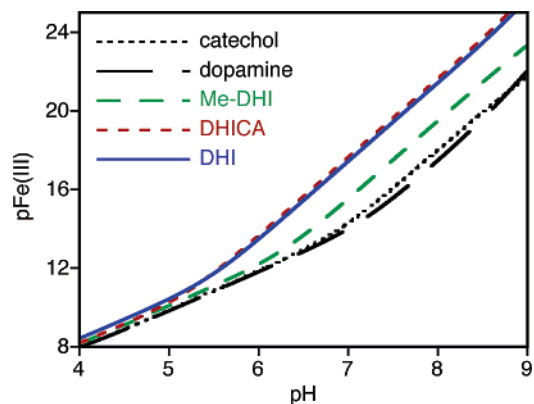

Figure 5. Plot of pFe(III) versus pH for model NM ligands: calculated for $[L]_{tot} = 10^{-5}$ M and $[Fe(III)]_{tot} = 10^{-6}$ M.
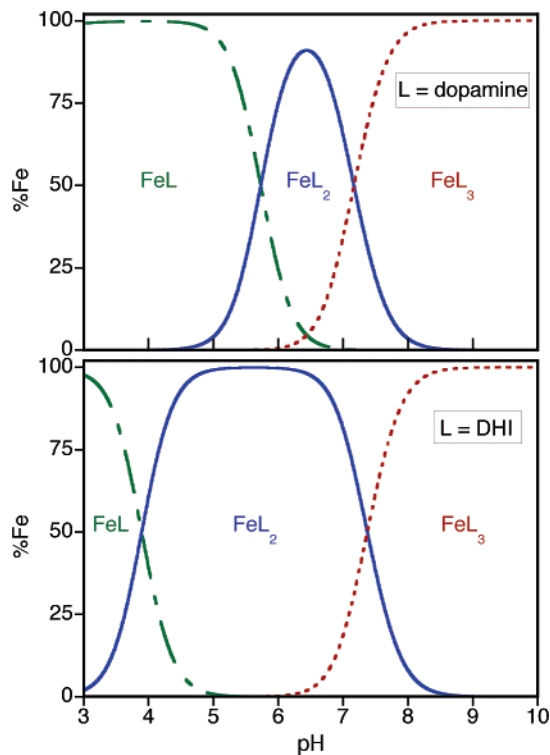

Figure 6. Calculated species distribution for Fe(III) complexes of dopamine (top) and DHI (bottom). Conditions as described in Figure 3.

mitter itself. In addition, the speciation curves shown in Figure 6 demonstrate that the bis FeL_2 species persists over a much wider pH range for DHI (and DHICA) compared to dopamine. It is also important to keep in mind that neuromelanin is a polymer composed of these monomer units and that the chelating possibilities of the polymer will influence the coordination chemistry in still unpredictable ways. Incorporation of metal ions into these polymers can also attenuate the redox behavior of melanin by altering the ratio of catechol, semiquinone, quinone, and quinoneimine functionalties, which in turn can affect whether melanin acts biologically as a pro- or antioxidant.[31,59]

The results of the current study provide a reasonable estimate for the affinity of discrete dihydroxyindole units that might be exposed on the periphery of the melanin

(59) Gidanian, S.; Farmer, P. J. *J. Inorg. Biochem.* **2002**, *89*, 54−60.

granule. According to the hypothesis that iron-saturated NM promotes oxidative damage, the low-affinity sites would become occupied as iron concentrations increase in the substantia nigra. Several factors, such as redox potential and the availability of open coordination sites on the metal, influence the ability of an Fe complex to promote OH$^{\bullet}$ formation from H_2O_2. Whether Fe coordinated as mono, bis, or tris dihydroxyindole complexes can promote OH$^{\bullet}$ formation via Fenton chemistry remains to be fully elucidated.[60]

A recent study showed that melanin biosynthesis can be induced by exposing certain cell types in culture to L-dopa to provide pigment that is indistinguishable from human NM.[30] Furthermore, pigment synthesis was inhibited by treatment with the iron chelator desferrioxamine, strongly suggesting that NM biosynthesis is iron dependent.[30] Preliminary oxidation studies described here show that iron accelerates the air oxidation of DHI and particularly DHICA. Although the mechanism of oxidation has not been investigated in detail here, possible scenarios include oxygen activation occurring either directly at the iron center or directly at a ligand that is activated via ligand−metal charge transfer from Fe(III)−catechol to Fe(II)−semiquinone.[61] Reactive intermediates from such a ligand-activation oxida-

tion could readily polymerize to form the insoluble black precipitate observed. If discrete Fe−dopamine or Fe−DHI complexes assemble prior to oxidative polymerization, the coordination compounds themselves might direct or template the architecture of the pigment differently from the metal-free precursors. The current study reveals that, although the tris Fe(III) complexes are the most stable, it is the formation of the bis species that is more favorable under the neutral to acidic conditions expected in and around NM granules. How these different coordination complexes might influence the ultimate connectivity, structure, and reactivity of the final pigment remains an open question.

Supporting Information Available: Spectral curves from the anaerobic pH-dependent spectrophotometric titrations of DHICA and Me-DHI with Fe(III) and lists of the models used for data fitting and refinement of the pH dependent spectrophotometric titrations. This material is available free of charge via the Internet at http://pubs.acs.org.

IC060014R

(60) Novellino, L.; Napolitano, A.; Prota, G. *Chem. Res. Toxicol.* **1999**, *12*, 985−992.

(61) Que, L.; Ho, R. *Chem. Rev.* **1996**, *96*, 2607−2624.